Recent Advances in Finite Element Methods for Structural Acoustics

Dr. Saikat Dey

Code 7130, Naval Research Laboratory, Washington D.C. USA

(On contract from SFA Inc. Crofton, Maryland, USA)

NIST Colloquium: March 28, 2006

OUTLINE

STARS3D: Software infrastructure for modeling *St*ructural *A*coustic *R*adiation and *S*cattering in *3D*.

Part-I Overview of *STARS3D*

- features, applications
- mathematical foundation
- p-approximations for numerically dispersive problems

Part-II *A-posteriori* Error Analysis

- sub-domain residual estimator
- effectivity indices

Part-III Scalable Parallelization

- stagewise concurrency, parallel multi-frontal, FETI-DP
- accuracy, scalability (efficiency) results on DoD HPC

Closing remarks and feedback

Application Areas

Structural acoustic response of elastic-fluid systems:

- Elastodynamics, eigen-analysis
- Interior noise analysis
- Radiation and scattering of waves exterior to elastic (rigid) structures
- Scattering from buried objects
- Acoustic transmission-loss modeling for sandwiched-honeycomb panels

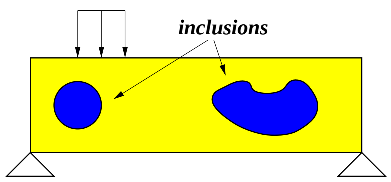

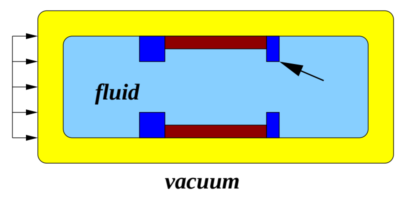

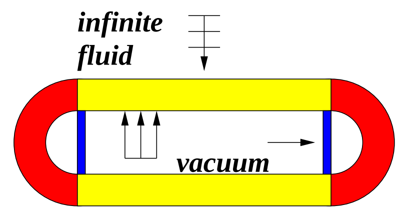

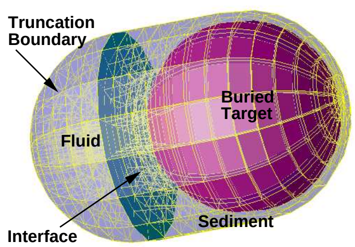

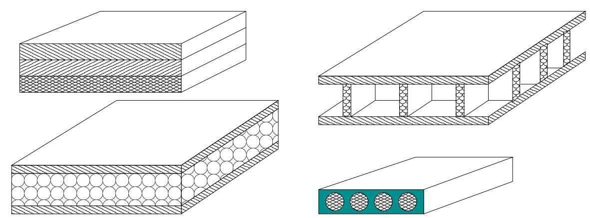

3D Composite Panel

STARS3D: Technical Capabilities

- 3D domain of arbitrary shape and complexity
- Support for multiple elastic and fluid regions
- Adaptable *hp*-finite/infinite element approximations
- Acoustic finite and infinite elements
- Perfectly Matched Layer (PML) approximations
- Linear isotropic three-dimensional elasticity
- Residual-based *a-posteriori* error estimation
- State-of-the-art parallel multi-frontal solver (NRL, MUMPS)
- Scalable domain-decomposition (*FETI*) algorithms
- Parallel execution in single and multi-frequency setting

General infrastructure supports wide range of applications.

Computational Domain Description

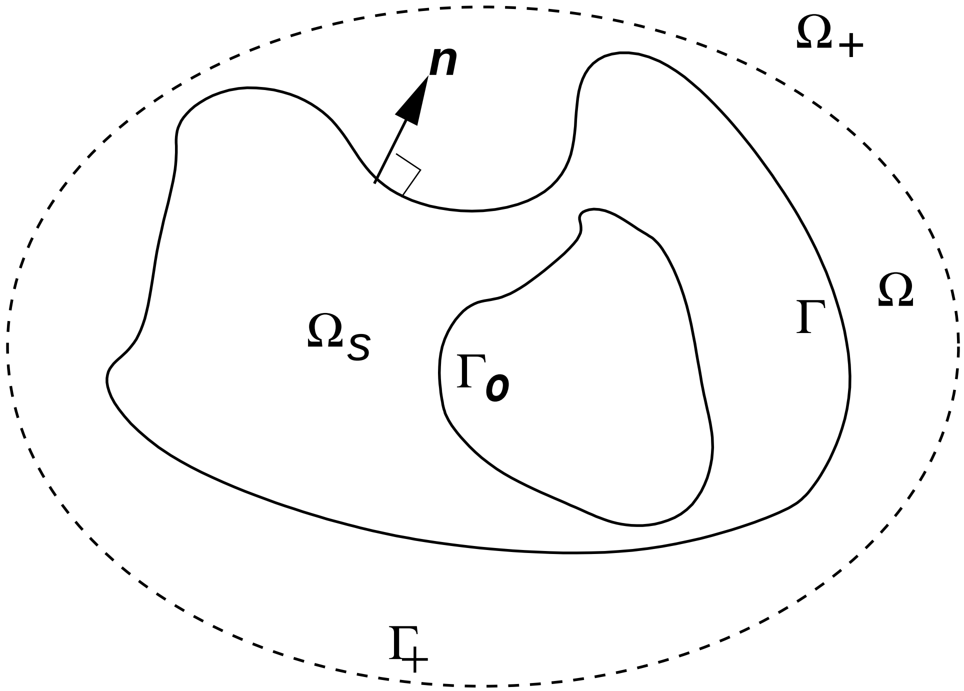

Fluid may fill structure exterior and/or interior.

Model Problem: Strong-form

$$\sigma_{jk,k} + \rho_s \omega^2 u_j = 0 \quad \text{in } \Omega_s$$

$$\phi_{,kk} + \frac{\omega^2}{c^2}\phi = 0 \quad \text{in } \Omega_f,$$

$$\sigma_{kj} n_j = h_k \quad \text{on} \quad \Gamma_h,$$

$$\sigma_{jk} n_k = -\left(\phi + \phi_0\right) n_j \quad \text{on } \Gamma,$$

$$\frac{\partial\left(\phi + \phi_0\right)}{\partial n} = \rho_f \omega^2 u_k n_k \quad \text{on } \Gamma, \quad \text{and}$$

$$\lim_{r\to\infty} r\left[\frac{\partial \phi}{\partial r}(r\hat{\mathbf{e}}) - i\frac{\omega}{c}\phi(r\hat{\mathbf{e}})\right] = 0, \quad \text{uniformly } \forall\, |\hat{\mathbf{e}}| = 1.$$

$i = \sqrt{-1}$

Abstract Variational Framework

$$a_s(\mathbf{u}, \mathbf{v}, \phi) = b_s(\mathbf{v}),$$
$$a_f(\phi, \psi, \mathbf{u}) + a_f^+(\phi^+, \psi^+) = b_f(\psi)$$

$$\mathcal{B}_{11}(\mathbf{u}, \mathbf{v}) + \mathcal{B}_{12}(\phi, \mathbf{v}) = \ \mathcal{L}_1(\mathbf{v})$$
$$\mathcal{B}_{21}(\mathbf{u}, \psi) + \mathcal{B}_{22}(\phi, \psi) + \ \mathcal{B}_{22}^+(\psi+, \psi^+) = \mathcal{L}_2(\psi)$$

	$\mathcal{B}_{11}$	$\mathcal{B}_{22}$	$\mathcal{B}_{12}$	$\mathcal{B}_{22}^+$
Exterior Acoustics	$\Uparrow$	$\Uparrow$	$\Uparrow$	$\Uparrow$
Interior Acoustics	$\Uparrow$	$\Uparrow$	$\Uparrow$	
Elastodynamics	$\Uparrow$			

Model Problem: Variational-form

$$a_s(\mathbf{u},\mathbf{v}) = \int_{\Omega_s} \left[v_{(j,k)} C_{jklm} u_{(l,m)} - \omega^2 \rho_s v_k u_k \right] \, d\Omega + \int_{\Gamma} \phi n_k v_k \, d\Gamma$$

$$a_f(\phi,\psi) = \int_{\Omega} \left[\phi_{,k} \psi_{,k} - \frac{\omega^2}{c^2} \phi \psi \right] \, d\Omega - \omega^2 \rho_f \int_{\Gamma} \psi n_k u_k \, d\Gamma$$

$$a_f^{+}(\phi^{+},\psi^{+}) = \lim_{S \to \infty} \left(\int_{\Omega_{RS}} \left[\nabla \phi^{+} \cdot \nabla \psi^{+} - \frac{\omega^2}{c^2} \phi^{+} \psi^{+} \right] \, d\Omega - i \frac{\omega}{c} \int_{\Gamma_{+}} \phi^{+} \psi^{+} \, d\Gamma \right)$$

$$b_s(\mathbf{v}) = - \int_{\Gamma} \phi_0 n_j v_j \, d\Gamma + \int_{\Gamma_h} h_j v_j d\Gamma$$

$$b_f(\psi) = \int_{\Gamma} \frac{\partial \phi_0}{\partial n} \psi \, d\Gamma$$

Computed Quantities of Interest

- interior pressure: ϕ
- wet-surface velocity (normal displacement): ωu_n
- stress (σ_{ij})
- far-field pressure form/pattern:

$$\phi_\infty(\hat{\mathbf{x}}) = \frac{1}{4\pi}\int_\Gamma \left[\frac{\partial\phi}{\partial n}(\mathbf{y}) + \ Ik\mathbf{n}(\mathbf{y})\hat{\mathbf{x}}\ \phi(\mathbf{y})\right] e^{-Ik\hat{\mathbf{x}}\ \mathbf{y}} d\Gamma(\mathbf{y})$$

  – Γ is any closed surface enclosing Ω_s,
  – $|\hat{\mathbf{x}}| = 1$

Infrastructure Overview

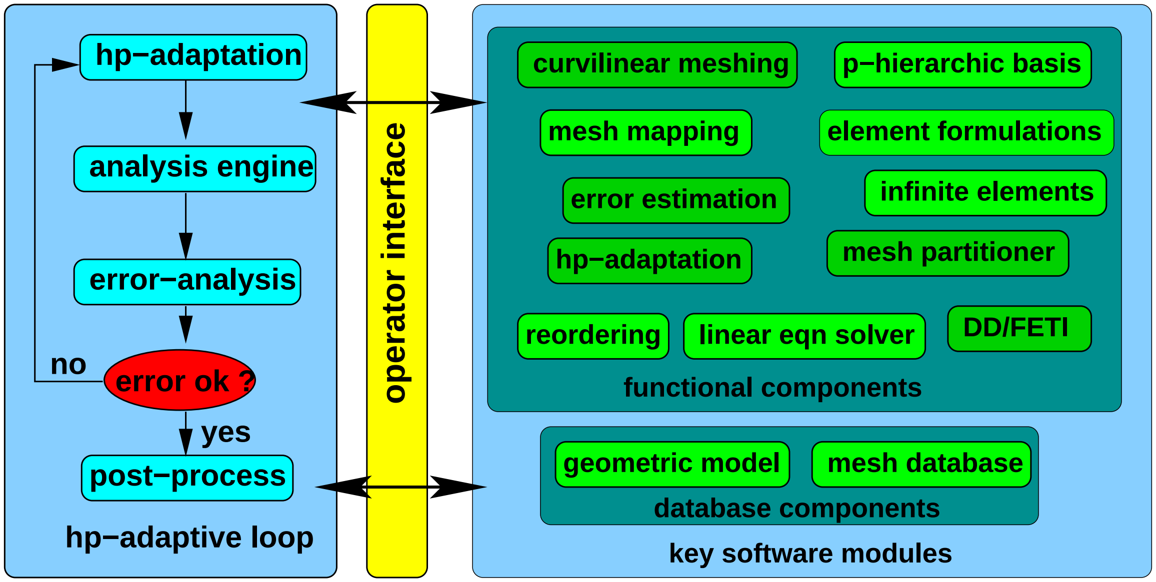

- Object-oriented, modular and extensible
- Supports arbitrary, 3D, geometric domains
- General-purpose Problem Solving Env. for PDE's

Approximation Issues

Why adaptable *hp*-FEM ?

Error control in FEM approximations:

1. *h*-refinement: element size subdivision, algebraic convergence, suitable near *singularities* and *discontinuities*

2. *p*-refinement: polynomial-degree escalation, exponential convergence, suitable for *smooth* solutions

3. *hp*-refinement: enables exponential convergence for problems with singularities/discontinuities

Approximation Improvement

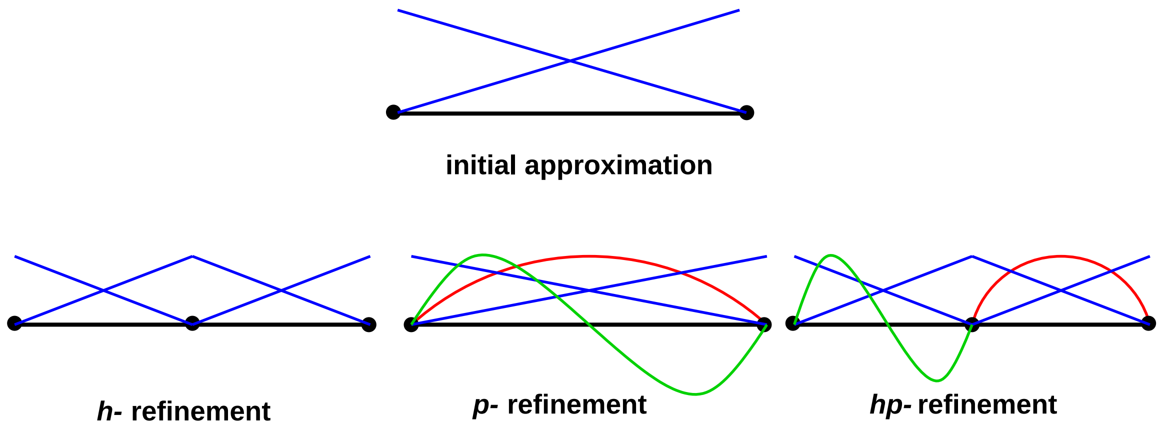

hp-adaptability enables:

- feedback-based approximation improvement
- smarter (optimal) error control: low p, smaller h near singularities
- preserves exponential convergence for properly designed meshes

Issues in Mid-to-High Frequency regime

How to control dispersion (*pollution*) error ?

Dispersion error analysis:

- *wavenumber*: $k = \frac{2\pi}{\lambda}$
- linear approximation: $hk < 1 \Rightarrow \frac{1}{h} > \frac{2\pi}{\lambda}$

  $\approx$ 10 elements per wavelength
- high-order approximation: $\frac{hk}{2p} < 1 \Rightarrow \frac{1}{h} > \frac{\pi}{p\lambda}$

  fewer elements per wavelength

Exponential *p*-convergence: Interior Problem

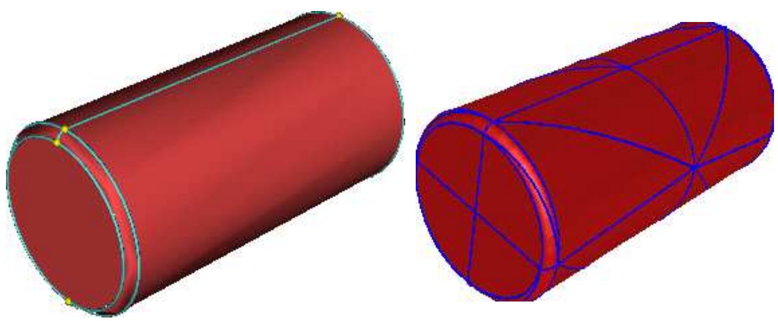

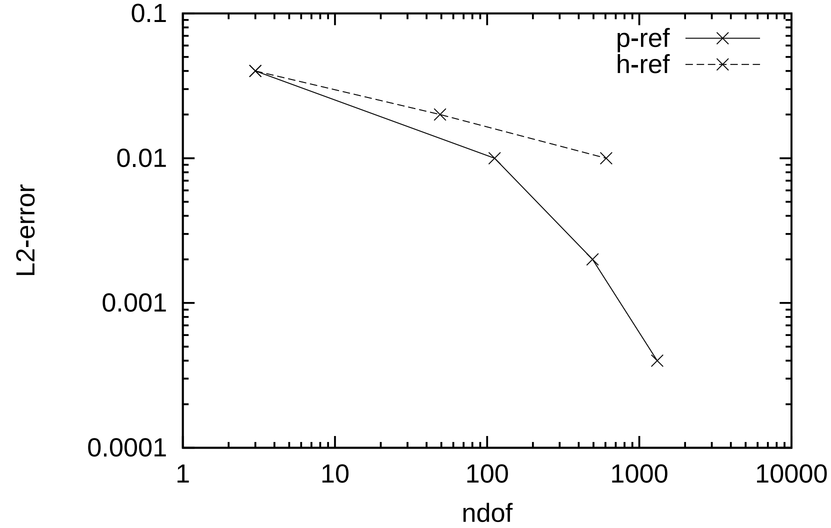

Application: ATC Eigen Analysis

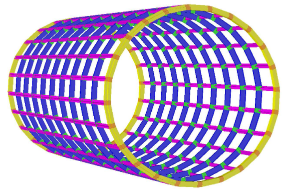

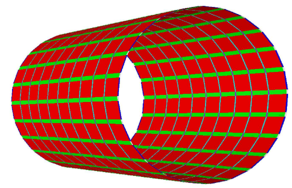

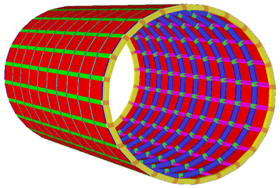

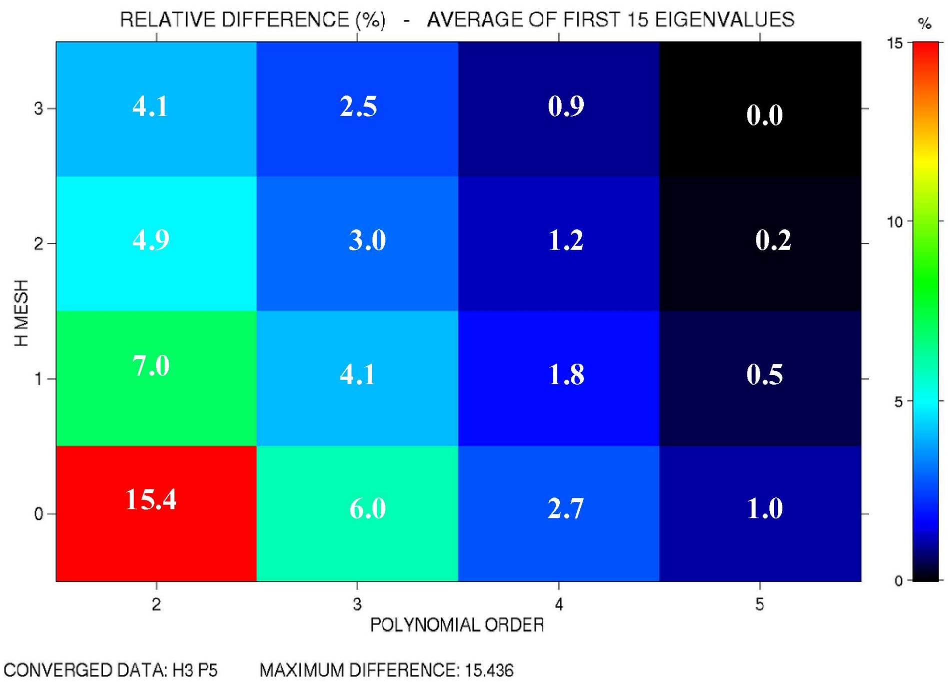

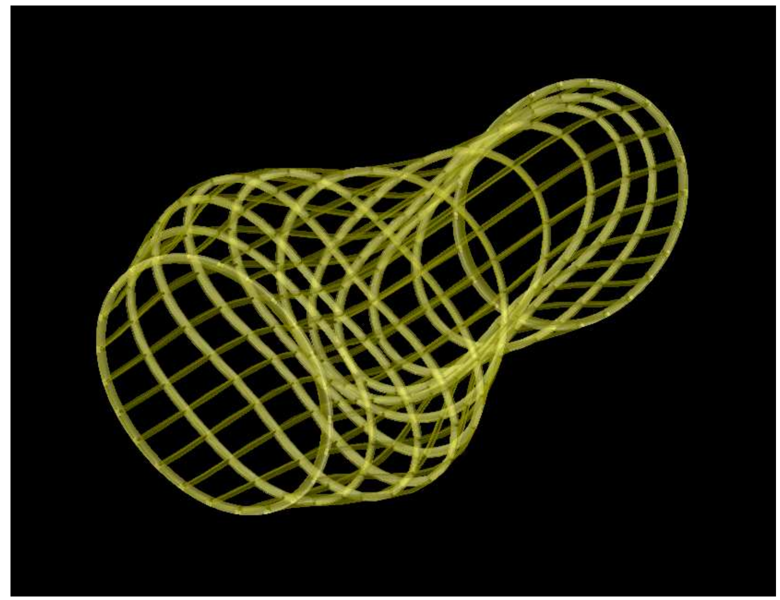

Application: Interior acoustics

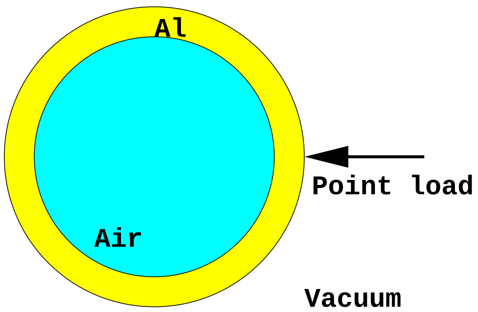

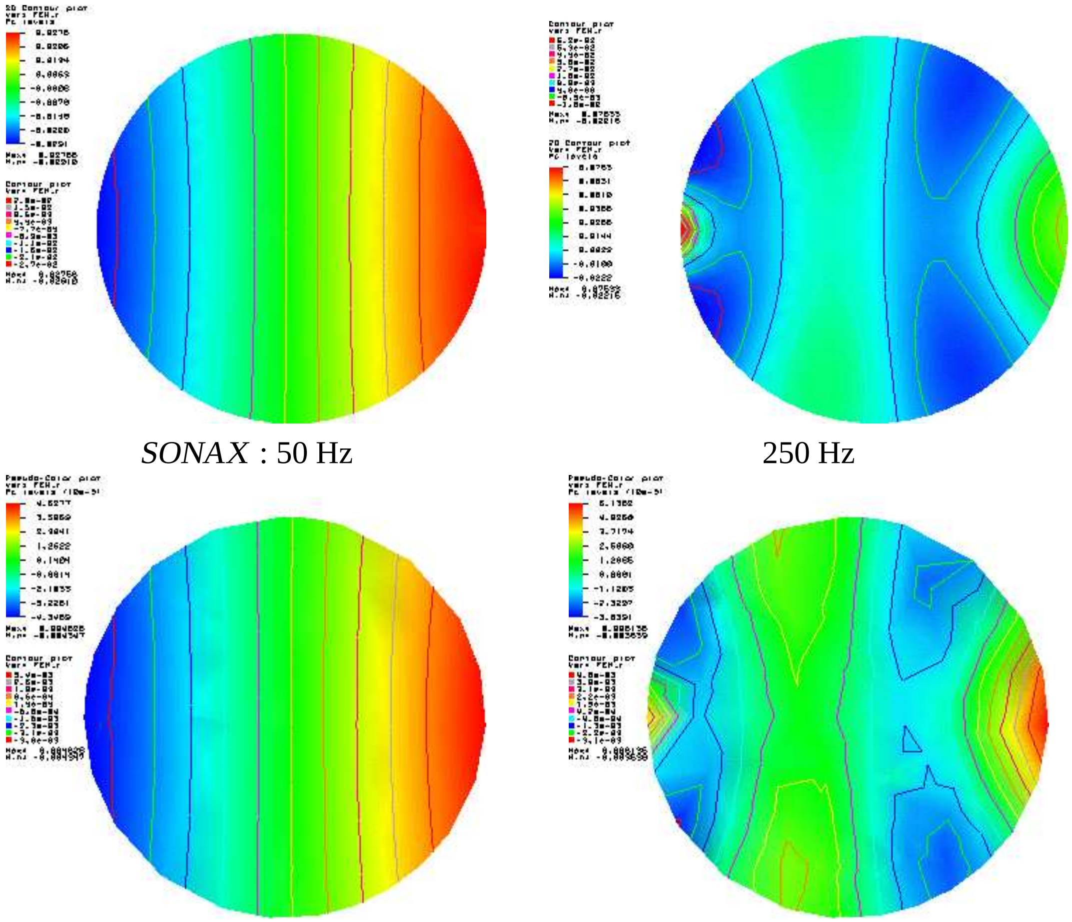

SONAX : 50 Hz

250 Hz

STARS3D : 50 Hz

250 Hz

Applications: Honeycomb Beam Predictive Validation

Courtsey:NASA Langley Research Center

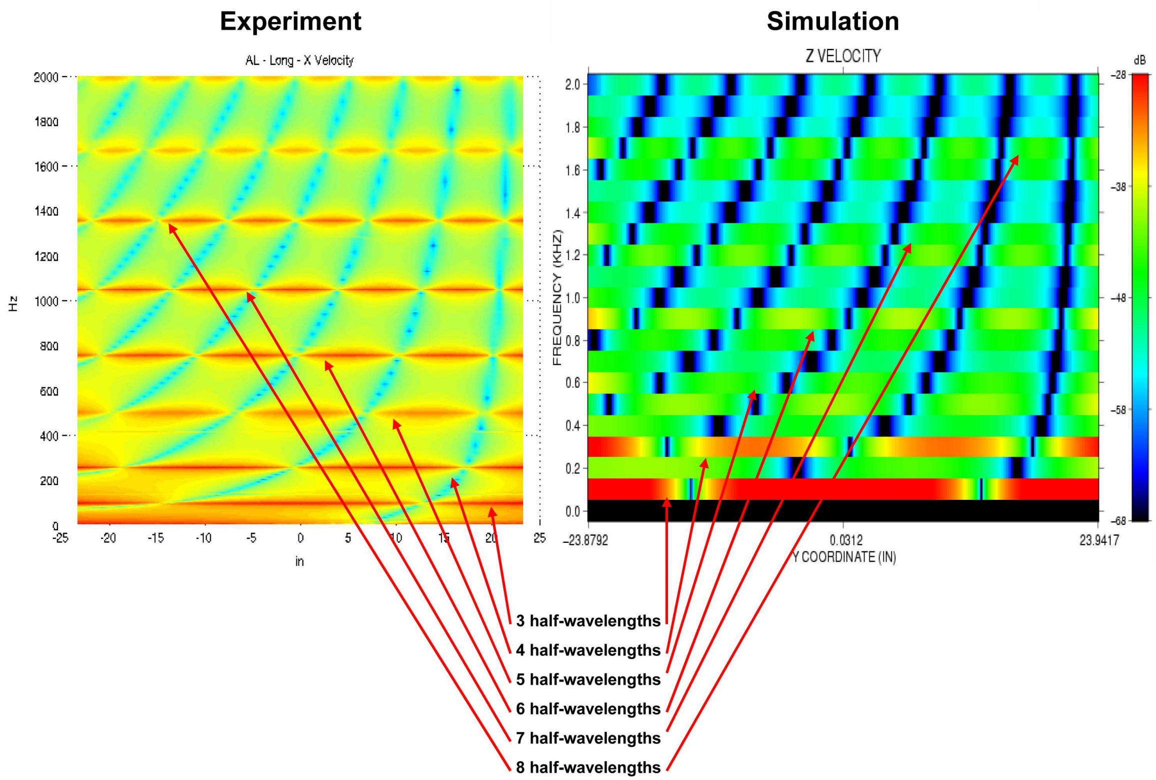

Colors *not* to same scale

Application: Acoustics Transmission Loss

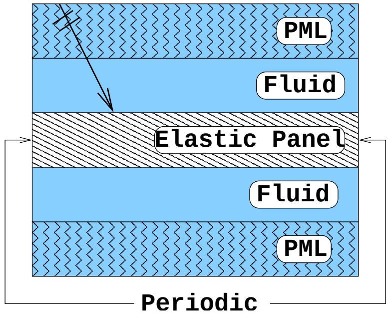

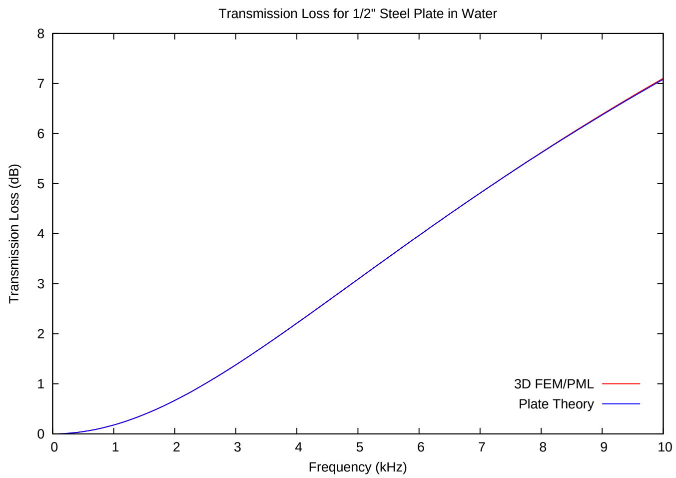

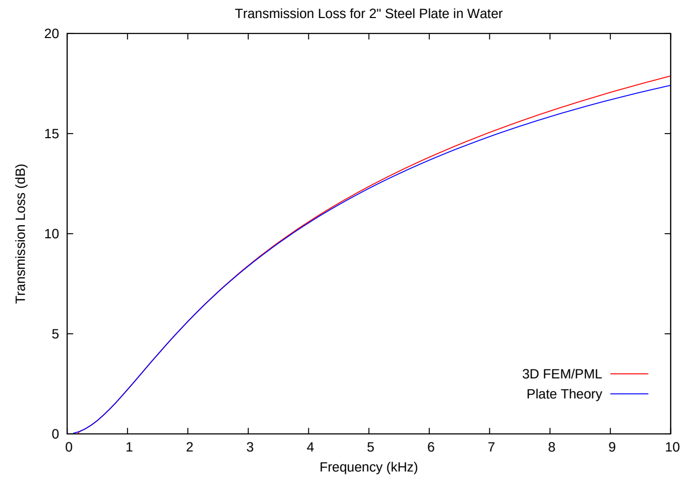

Model 0.5 inch 2.0 inch

Frequency-sweep validation against analytic (plate-theory) result

p-Hierarchic Basis Functions

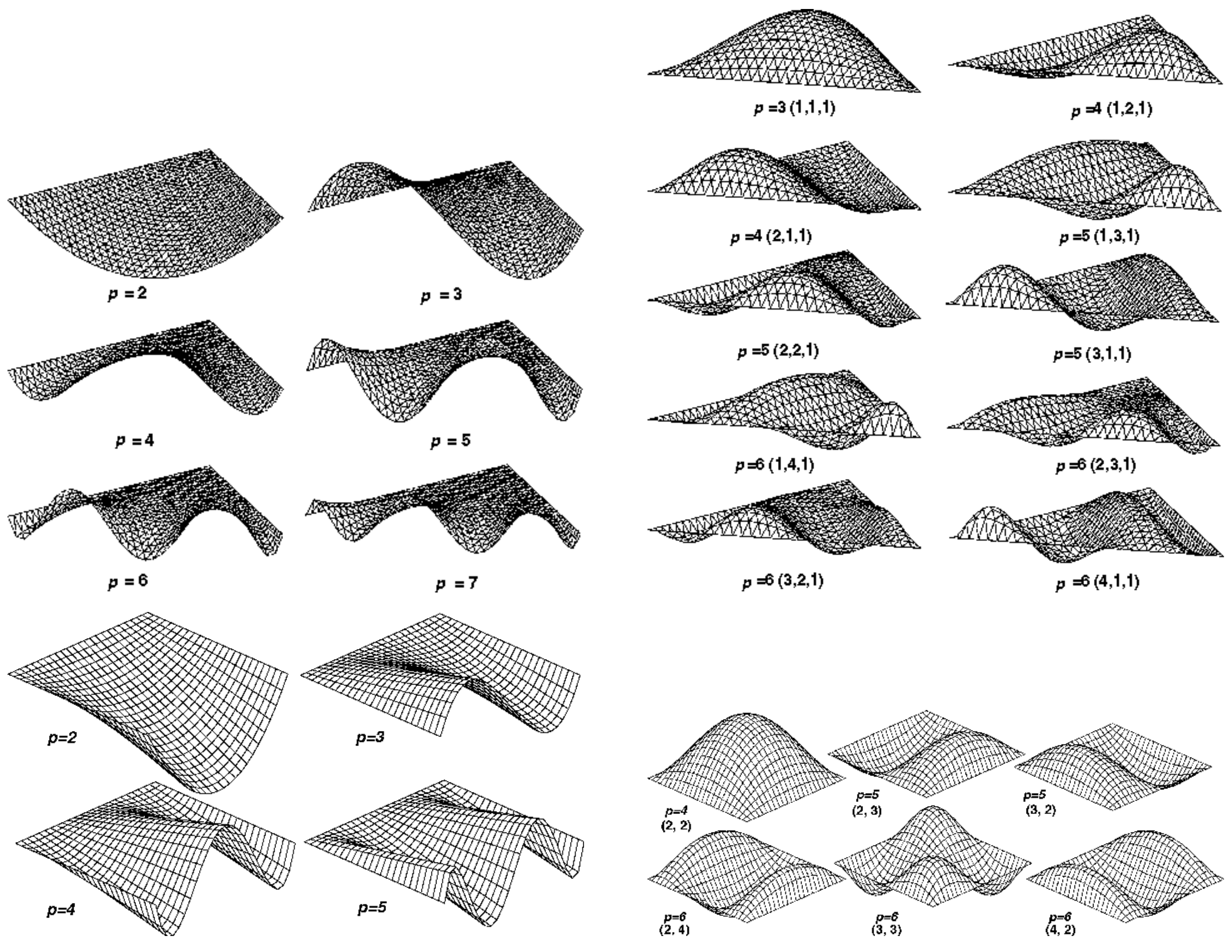

Topology-Based basis function decomposition

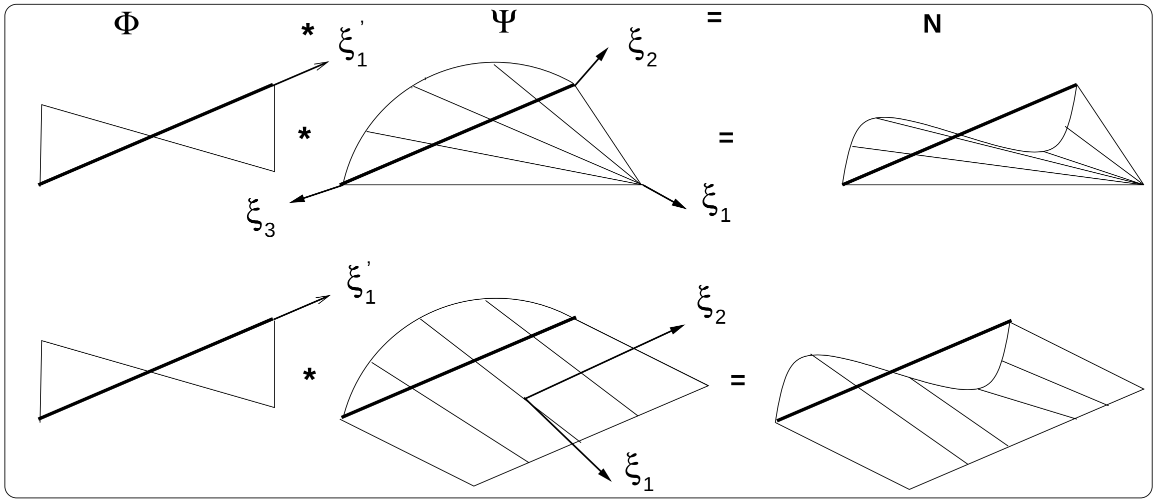

- $N = \psi(\xi) * \phi(\xi')$
- $\phi(\xi')$ associated only with mesh entity (V,E,F,R)
- $\psi(\xi)$ blends $\phi(\xi')$ over the element domain
- ξ - element coordinates, $\xi' = f(\xi)$ - entity coordinates

Advantages of Topology-Based decomposition

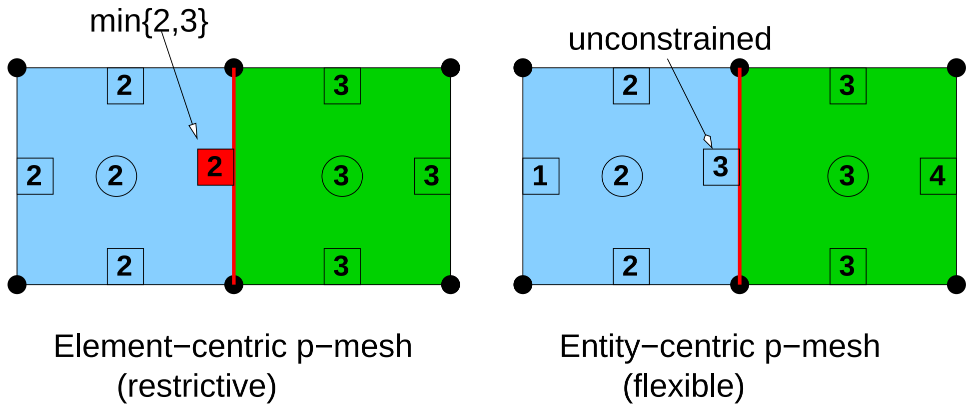

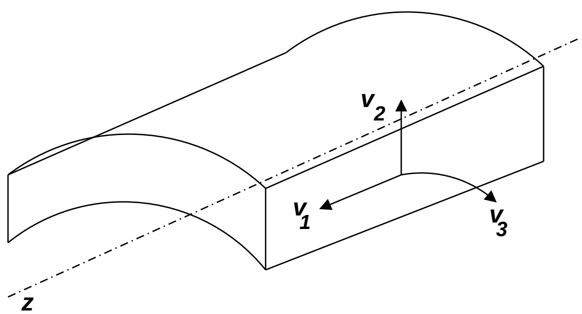

- totally flexible degree specification; C^0 by construction
- anisotropic, variable-order *p*-adaptivity
- easy addition of: new basis (ϕ), new elements (ψ)
- independent (p_1, p_2, p_3) along (v_1, v_2, v_3)

Flexible, unconstrained p-adaptation!

A-posteriori error estimation

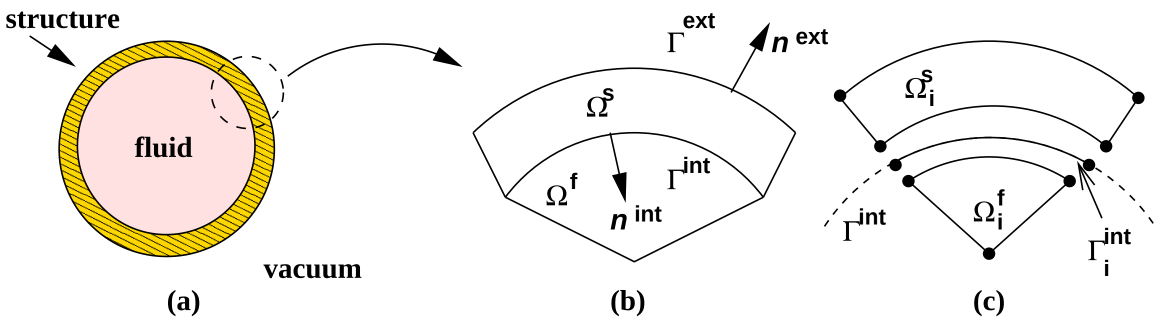

- three-dimensional, interior acoustics
- subdomain-based residual estimator
- estimates of error in ϕ and u_r in global L_2 and H^1 norms
- effectivity indices as a function of ka and p

p-Error Analysis Framework

Primary problem:

$$\mathcal{B}_{11}(u_j^{(p_s)}, v_j) + \mathcal{B}_{12}(\phi^{(p_f)}, v_j) = \mathcal{L}_1(v_j)$$

$$\mathcal{B}_{21}(u_j^{(p_s)}, \psi) + \mathcal{B}_{22}(\phi^{(p_f)}, \psi) = \mathcal{L}_2(\psi)$$

Define error: $e_{u_j} = u_j - u_j^{(p_s)}$ and $e_\phi = \phi - \phi^{(p_f)}$

Residual equations:

$$\mathcal{B}_{11}(e_{u_j}, v_j) + \mathcal{B}_{12}(e_\phi, v_j) = \mathcal{L}_1(v_j) - \mathcal{B}_{11}(u_j^{(p_s)}, v_j) - \mathcal{B}_{12}(\phi^{(p_f)}, v_j)$$

$$\mathcal{B}_{21}(e_{u_j}, \psi) + \mathcal{B}_{22}(e_\phi, \psi) = \mathcal{L}_2(\psi) - \mathcal{B}_{21}(u_j^{(p_s)}, \psi) - \mathcal{B}_{22}(\phi^{(p_f)}, \psi)$$

Global Residual Estimator: *GRE*

$$\mathcal{B}_{11}(e_{u_j}^{p_s'}, v_j) + B_{12}(e_{\phi}^{p_f'}, v_j) = \mathcal{L}_1(v_j) - \mathcal{B}_{11}(u_j^{(p_s)}, v_j) - \mathcal{B}_{12}(\phi^{(p_f)}, v_j)$$

$$\mathcal{B}_{21}(e_{u_j}^{p_s'}, \psi) + B_{22}(e_{\phi}^{p_f'}, \psi) = \mathcal{L}_2(\psi) - \mathcal{B}_{21}(u_j^{(p_s)}, \psi) - \mathcal{B}_{22}(\phi^{(p_f)}, \psi)$$

$$\mathcal{E}_{u_j,*(\Omega_s)}^{GRE} \stackrel{\text{def}}{=} \sqrt{\sum_{\tau \in \Delta_h} || e_{u_j}^{h,p_s',q_s'} ||_{*(\tau)}^2} \qquad \mathcal{E}_{\phi,*(\Omega_f)}^{GRE} \stackrel{\text{def}}{=} \sqrt{\sum_{\tau \in \Delta_h} || e_{\phi}^{h,p_f'} ||_{*(\tau)}^2}$$

- enriched-subspace: $p_s' > p_s$ and $p_f' > p_f$
- $p_s' \to \infty$, and $p_f' \to \infty \quad \Rightarrow$ *exact* error
- *expensive*, but useful verification tool

Subdomain Residual Estimator: *SRE*

Definitions:

- φ_X is global piecewise linear basis for vertex X,
- support for φ_X:

$$\varpi_X = supp(\varphi_X) = \bigcup_{\substack{\tau \in \Delta_h \\ X \in \partial\tau}} \tau$$

- in 3D, ϖ_X is the closure of mesh regions connected vertex to X
- φ_X form a *partition of unity* and vanish on $\partial\varpi_X$
- natural setup for a *Dirichlet*-type estimator

Subdomain Residual Estimator: *SRE*

$$\mathcal{U}_0^{h,p'_s,q'_s}(\varpi_X) \stackrel{\text{def}}{=} \left\{ v_j \in \mathcal{U}^{h,p'_s,q'_s}(\varpi_X) \middle| \; v_j|_{\partial\varpi_{X,D}} = 0 \right\}$$

$$\Phi_0^{h,p'_f}(\varpi_X) \stackrel{\text{def}}{=} \left\{ \psi \in \; \Phi^{h,p'_f}(\varpi_X) \middle| \; \psi|_{\partial\varpi_{X,D}} \; = 0 \right\}$$

$$\mathcal{B}_{11}(\hat{e}_{u_j}, v_j) + \mathcal{B}_{12}(\hat{e}_\phi, v_j) \; = \mathcal{L}_1(v_j) - \mathcal{B}_{11}(u_j^{(p_s)}, v_j) - \mathcal{B}_{12}(\phi^{(p_f)}, v_j)$$

$$\mathcal{B}_{21}(\hat{e}_{u_j}, \psi) + \mathcal{B}_{22}(\hat{e}_\phi, \psi) \; = \mathcal{L}_2(\psi) - \mathcal{B}_{21}(u_j^{(p_s)}, \psi) - \mathcal{B}_{22}(\phi^{(p_f)}, \psi)$$

$$\mathcal{E}^{SRE}_{u_j,*(\Omega_s)} \stackrel{\text{def}}{=} \sqrt{\sum_X \sum_{\tau \in \varpi_X} ||\hat{e}_{u_j}||^2_{*(\tau)}} \qquad \mathcal{E}^{SRE}_{\phi,*(\Omega_f)} \stackrel{\text{def}}{=} \sqrt{\sum_X \sum_{\tau \in \varpi_X} ||\hat{e}_\phi||^2_{*(\tau)}}$$

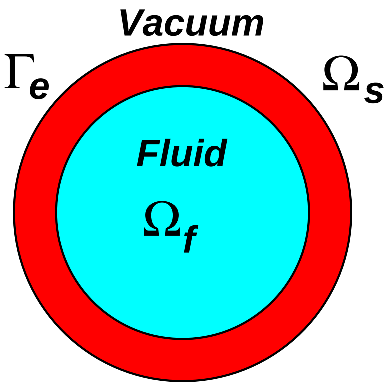

Error estimation: Numerical results

- semi-analytic reference solution[1] $u_{r,EX}$ and ϕ_{EX}
- effectivity indices

$$\eta^{EST}_{u_r,L^2(\Omega_s)} = \mathcal{E}^{EST}_{u_r,L^2(\Omega_s)} \Big/ ||u_{r,EX} - u_r^{h,p_s,q_s}||_{L^2(\Omega_s)}$$

$$\eta^{EST}_{\phi,L^2(\Omega_f)} = \mathcal{E}^{EST}_{\phi,L^2(\Omega_f)} \Big/ ||\phi_{EX} - \phi^{(p_f)}||_{L^2(\Omega_f)}$$

[1] Thanks to Dr. J. J. Shirron

Resonances in frequency response

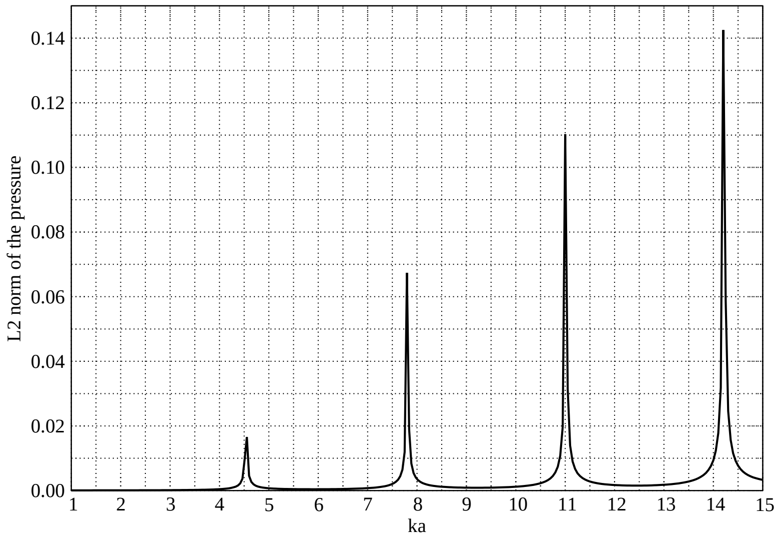

Pressure

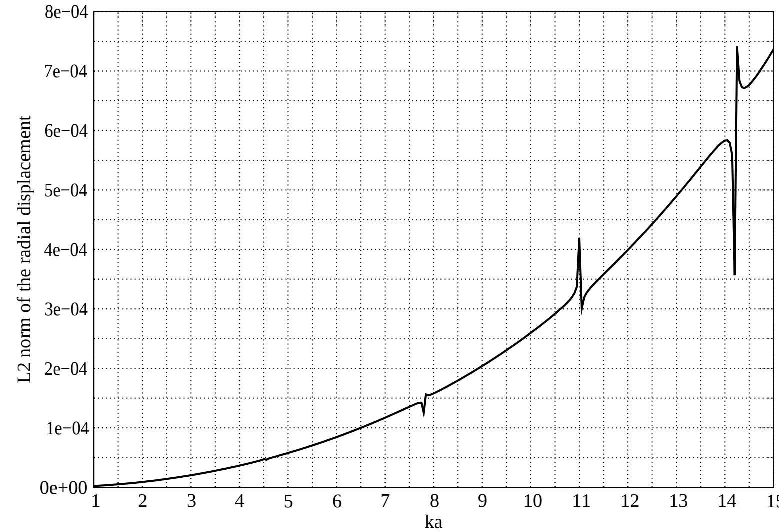

Radial displacement

- Input data:

$$c = 320ms^{-1},\ \rho_s = 7800Kgm^{-3},$$

$$\rho_f = 1.25Kgm^{-3},\ E = 2.0 \times 10^{11}Nm^{-2},\ \nu = 0.3.$$

Effectivity Indices for GRE

ka	Pressure	Radial displacement	ka	Pressure	Radial displacement
1	0.8377	0.9968	9	1.0418	0.6853
2	0.8030	0.9922	10	0.9242	0.6813
3	0.7721	0.9795	11	0.6510	0.1413
4	0.9163	0.9045	12	0.8200	0.8053
5	0.6518	0.9786	13	1.1207	0.6371
6	0.8590	0.9842	14	1.9303	0.0730
7	0.9302	0.8418	15	1.1247	0.4155
8	0.5115	0.2937			

- Numbers in red indicate ka is near resonant frequency

Effectivity Indices for Pressure using SRE

ka	$p_f = 2$	$p_f = 3$	ka	$p_f = 2$	$p_f = 3$
1	0.6924	0.3946	9	1.4693	0.8138
2	0.5990	0.6848	10	0.9220	1.0748
3	0.6846	0.4926	11	0.1131	0.0696
4	0.9740	1.1176	12	1.0447	0.7675
5	1.7748	1.2492	13	2.7795	0.7610
6	1.7382	1.0288	14	0.6469	0.1181
7	1.2310	0.6539	15	2.2464	0.7834
8	0.9351	0.2195			

Effectivity Indices for Radial displacement using SRE

ka	$p_s = 2$	$p_s = 3$	ka	$p_s = 2$	$p_s = 3$
1	1.0352	1.6593	9	0.4852	0.3191
2	1.0246	1.6493	10	0.3527	0.2341
3	1.0012	1.6226	11	0.0308	0.0103
4	0.9107	1.1214	12	0.1126	0.1225
5	0.9626	0.5435	13	0.2909	0.1194
6	0.9348	0.6421	14	0.0469	0.0153
7	0.7570	0.3314	15	0.1755	0.2583
8	0.2424	0.0927			

Brief Aside: Mesh Representation

AMD: Adaptable Mesh Database

- non-manifold, polymorphic topology
- on-the-fly application-adaptive topological adjacencies
- high-order geometry representation
- partitioned meshes
- mesh entities mapped to geometric and partition models
- tools to convert legacy (element-node) representations

Brief Aside: Mesh Partitioning

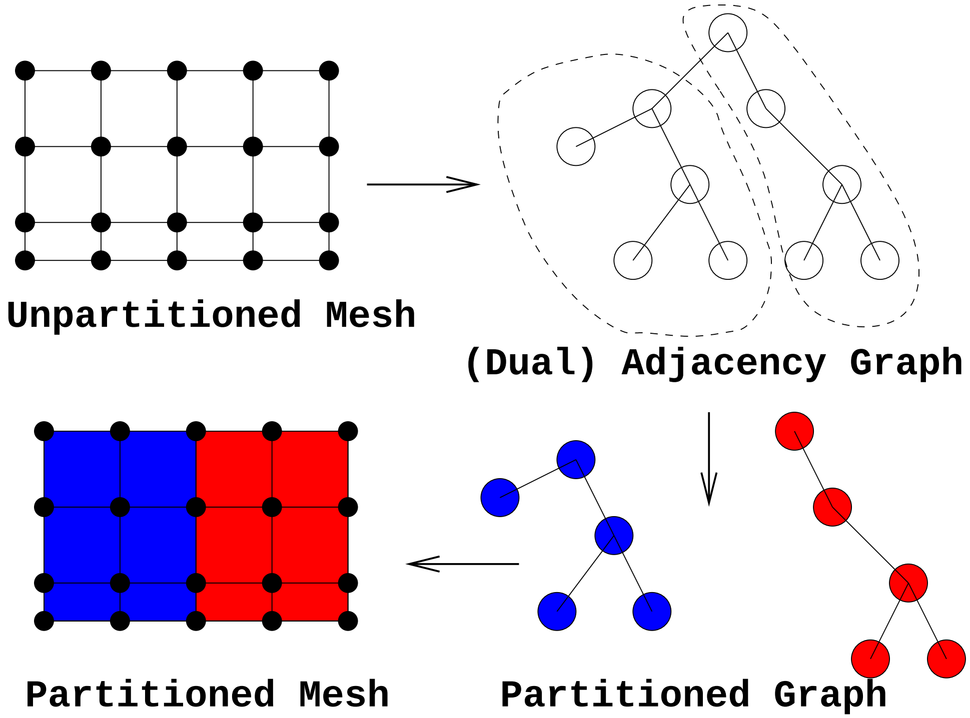

Alternative partitioning: greedy, octree-based, recursive-bisection-based etc.

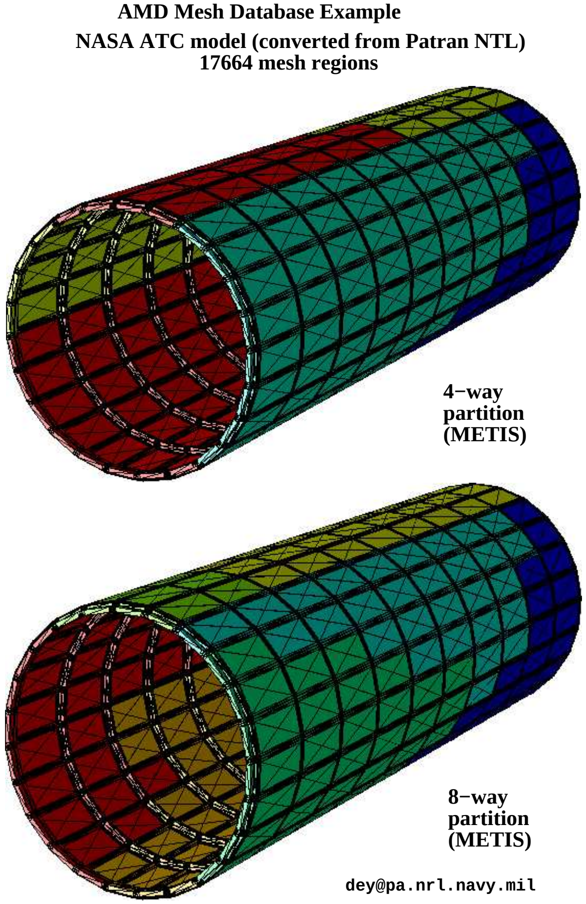
AMD Mesh Database Example
NASA ATC model (converted from Patran NTL)
17664 mesh regions
4−way
partition
(METIS)
8−way
partition
(METIS)
dey@pa.nrl.navy.mil

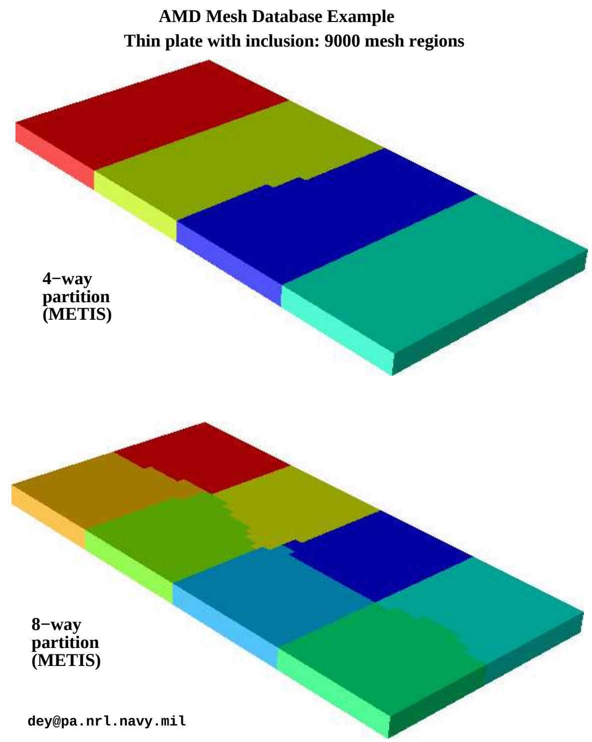
AMD Mesh Database Example
Thin plate with inclusion: 9000 mesh regions
4−way
partition
(METIS)
8−way
partition
(METIS)
dey@pa.nrl.navy.mil

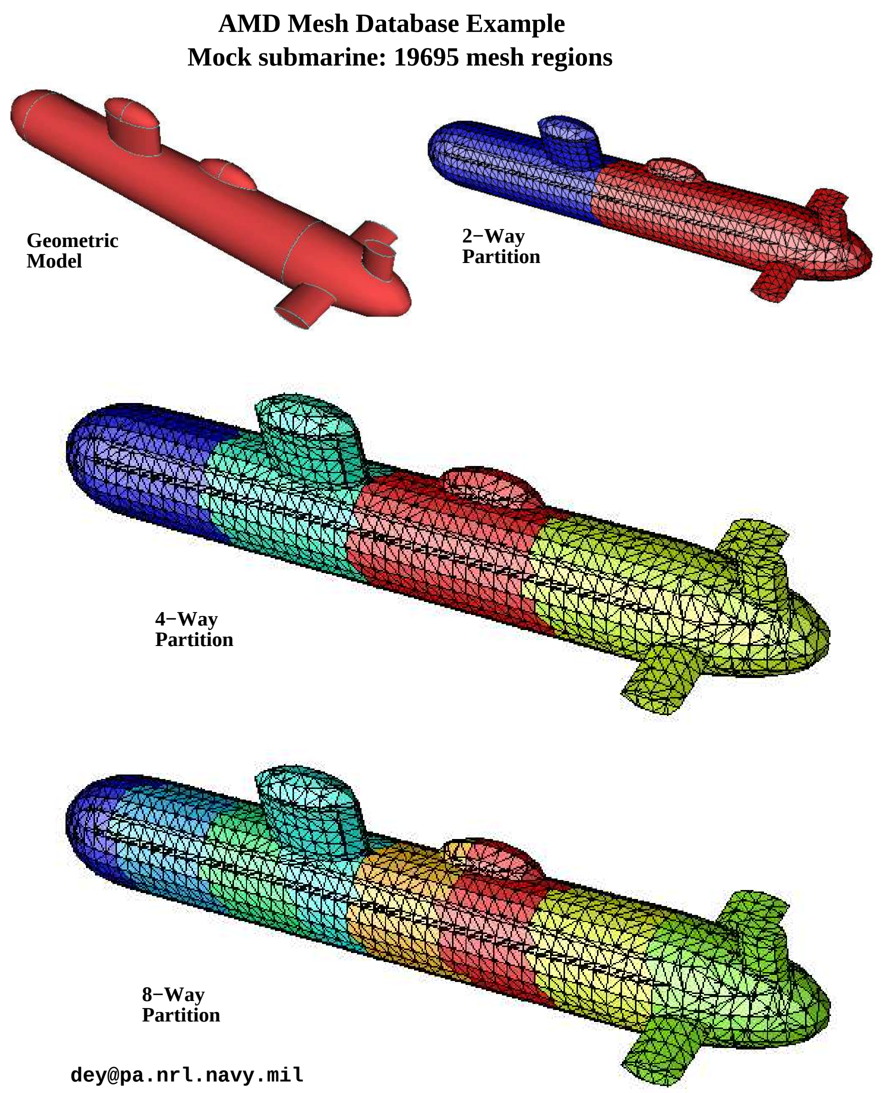
AMD Mesh Database Example
Mock submarine: 19695 mesh regions
Geometric
Model
2−Way
Partition
4−Way
Partition
8−Way
Partition
dey@pa.nrl.navy.mil

STARS3D: Scheme of Computation

Stage-1 Compute (cache) element-level matrices/vectors.
Stage-2 Assemble and solve global system of equations.
Stage-3 Post-process user-requested quantities of interest.

Single-frequency Execute Stage-1,2,3 once.
Multi-frequency Independent execution of Stage-1,2,3 for each frequency.

- *embarassingly parallel*
- Stage-1 cache reusable for fixed hp

STARS3D: Stage-1 Computation

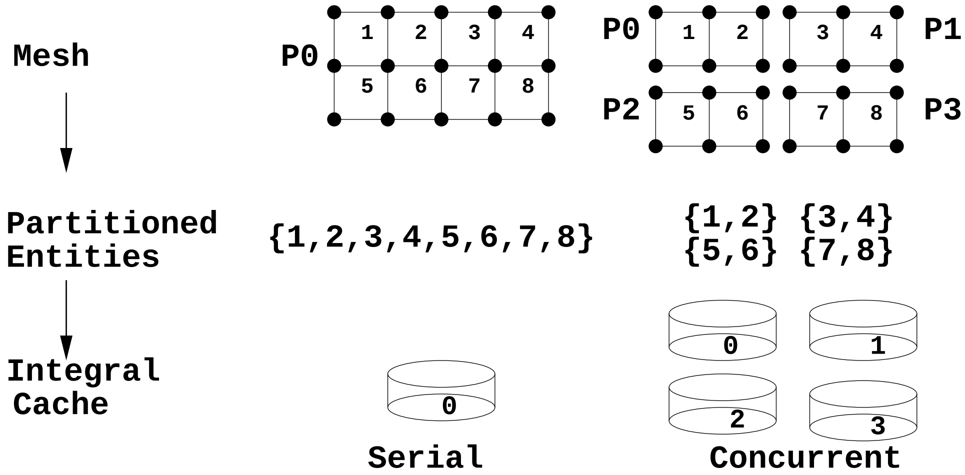

Each partition:

- Creates its own approximation (elements)
- Computes and caches element integrals for its approximation
- Naturally high scalability

STARS3D: Stage-2 Computation

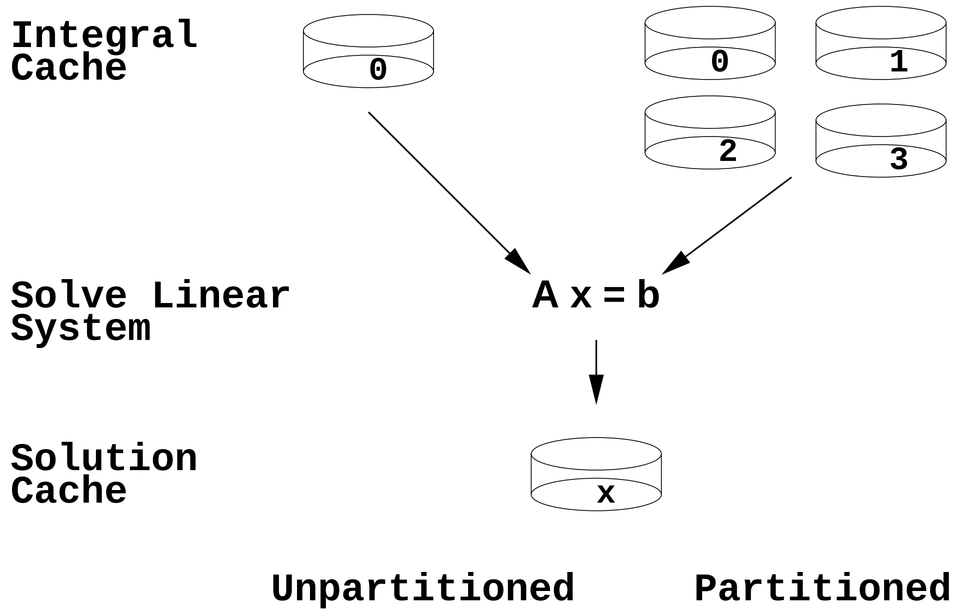

- Assembly process deals with (multiple) partition cache(s)
- Linear solve: highly irregular, data-dependent
- Challenging for scalable parallelization

STARS3D: Stage-3 Computation

Example

- Farfield projection
- Norm (error) computation
- Field output

Partitioned domain

- Global integrals broken into sum of partition integrals
- Processors compute for their assigned partition
- Global-reduce operation gets the final result

Parallel Scheme: Multi-Frequency

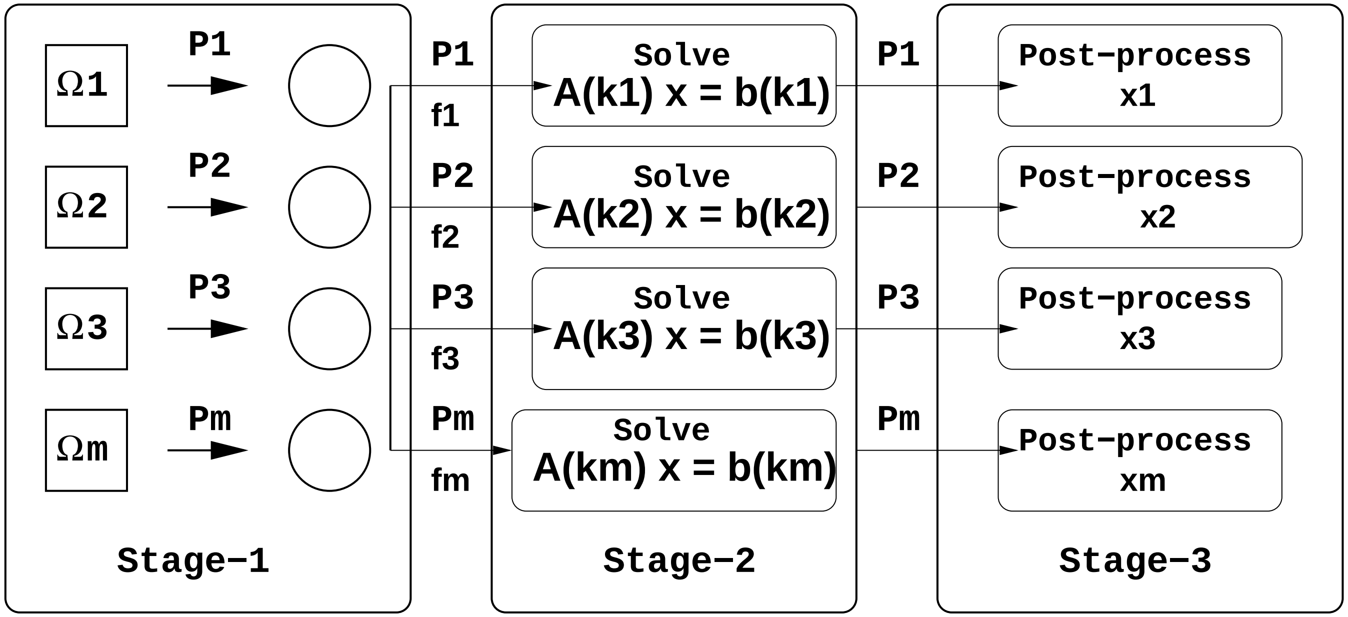

- Naturally high scalability
- Can use multi-frontal or FETI-DP for Stage-2

Single Frequency Parallel Multi-Frontal Performance

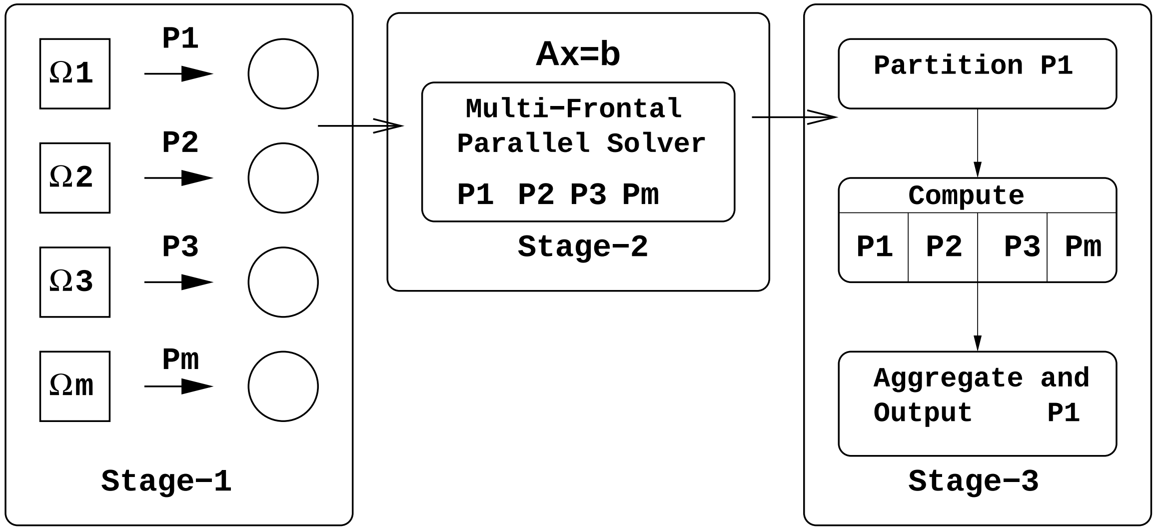

- Stage 1 and Stage 3 scales well
- Stage 2: Matrix-factoring highly irregular; rapidly decreasing concurrent work-load
- Parallel multi-frontal has limited scalability (4 to 8 processors)
- Example: 1.2M dofs, seepdup (effi ciency): 3.4/4 (85%), 4.8/8 (60%)
- Utilize scalable DD method: FETI-DP

FETI-DP

- Scalable domain decomposition scheme
- Independent solve of sub-domain problems ("Tearing" phase)
- Sub-domain solutions "interconnected" by Lagrange multipliers
- Two (Fine and Coarse) level iterative-substructuring scheme
  - Coarse problem by defining "corner" DOF at a global level
- Augmented FETI-DP
  - Enforce optional constraint on residuals at each iteration step

FETI-DP: The recipe itself is algebraic in nature

Large body of literature on FETI and its variants

FETI-DP Formulation

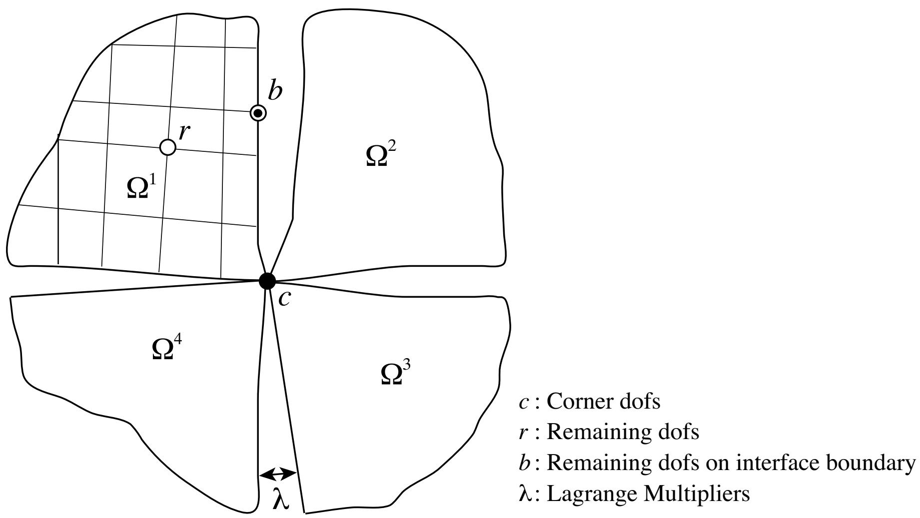

Subdomain equations:

$$K^s u^s = f^s \quad \Rightarrow \quad \begin{bmatrix} K^s_{rr} & K^s_{rc} \\ {K^s_{rc}}^T & K^s_{cc} \end{bmatrix} \begin{bmatrix} u^s_r \\ u^s_c \end{bmatrix} = \begin{bmatrix} f^s_r \\ f^s_c \end{bmatrix}$$

FETI-DP Formulation (*contd.*)

Subdomain interface continuity condition:

$$u_b^m - u_b^n = 0 \quad \text{on } \partial\Omega^m \cap \partial\Omega^n \quad \Rightarrow \quad \sum_{s=1}^{s=N} B_r^s u_r^s = 0$$

where B_r^s is a signed boolean matrix such that $B_r^s u_r^s = \pm u_b^s$

- Enforce continuity at the subdomain interfaces by *Lagrange Multipliers*

FETI-DP Formulation (*contd.*)

Interface problem by eliminating u_r^s and u_c^s:

$$\big(\underbrace{F_{rr}}_{Fine} + \underbrace{F_{rc}{K_{cc}^*}^{-1}{F_{rc}}^T}_{Coarse}\big)\lambda \;= d_r - F_{rc}{K_{cc}^*}^{-1}f_c^*$$

where

$$F_{rr} = \sum_{s=1}^{s=N} B_r^s {K_{rr}^s}^{-1} B_r^{sT}, \quad F_{rc} = \sum_{s=1}^{s=N} B_r^s {K_{rr}^s}^{-1} K_{rc}^s B_c^s$$

$$K_{cc}^* = \sum_{s=1}^{s=N} B_c^{sT} K_{cc}^s B_c^s - (K_{rc}^s B_c^s)^T {K_{rr}^s}^{-1} K_{rc}^s B_c^s$$

$$d_r = \sum_{s=1}^{s=N} B_r^s {K_{rr}^s}^{-1} f_r^s, \quad f_c^* = f_c - \sum_{s=1}^{s=N} B_c^{sT} {K_{rc}^s}^T {K_{rr}^s}^{-1} f_r^s$$

FETI-DP in STARS3D

- Works with higher order hierarchical basis and infinite elements
  - Lagrange multipliers enforce matching of coefficients of p-approximation
- Sparse multi-frontal solver to factorize subdomain matrices K_{rr}^{s}
- GMRES and GCR for iterative solution of the interface problem
- Lumped preconditioner: $\sum_{s=1}^{s=N} B_r^s K_{bb}^s B_r^{sT}$
- MPI-based implementation

First known application of FETI-DP to p- fi nite+infi nite element approximations in 3D

CHSSI Problem Set Overview

Single Frequency:

Problem 1 Exterior scattering from smooth elastic cylindrical shell
Problem 2 Exterior scattering from stiffened elastic cylindrical shell

Multiple Frequency:

Problem 3 Exterior scattering from smooth elastic spherical shell
Problem 4 Interior acoustics of fluid-filled elastic spherical shell
Problem 5 Interior acoustics of fluid-filled elastic cylindrical shell

Test problem	1	2	3	4	5
Problem type	exterior	exterior	exterior	interior	interior
Excitation	plane wave	plane wave	plane wave	elastic traction	elastic traction
Reference solution	numerical	numerical	analytical	analytical	numerical

DoD HPC Platforms Used

	SGI Altix 3900	SGI Origin 3800	Linux-Cluster	IBM p690 SP
OS	GNU/Linux	IRIX 6.5	GNU/Linux	AIX
Processors	IA64	MIPS R14000	IA32	Power 4+
Memory	Shared	Shared	Distributed	Distributed
Compilers	GNU	MIPS	GNU	IBM
	M1	M2	M3	M4

STARS3D easily ports to any platform that has:

- *Unix*-like OS, `GNU-make`, `bash`
- ANSI C, F77 and (optionally) F90 compilers
- MPI and (optionally) OpenMP support

Multi-frequency (multi-frontal) Parallel Scalability

P3				
n_p	M1	M2	M3	M4
2	2.0 (1.00)	2.0 (1.00)	2.0 (1.00)	2.0 (1.00)
4	3.8 (0.95)	3.3 (0.81)	4.0 (1.00)	3.4 (0.84)
8	7.5 (0.94)	6.7 (0.83)	7.6 (0.95)	7.5 (0.93)
16	14.2 (0.87)	16.1 (1.00)	15.9 (0.99)	14.3 (0.90)
32	19.9 (0.62)	20.3 (0.63)	29.4 (0.92)	23.4 (0.73)
P4				
n_p	M1	M2	M3	M4
2	2.0 (1.00)	2.0 (1.00)	2.0 (1.00)	2.0 (1.00)
4	4.0 (1.00)	3.9 (0.97)	2.8 (0.69)	3.4 (0.84)
8	8.0 (1.00)	7.8 (0.97)	4.8 (0.60)	6.5 (0.81)
16	15.9 (0.99)	15.0 (0.94)	14.3 (0.89)	12.1 (0.75)
32	31.0 (0.97)	29.0 (0.91)	18.7 (0.58)	24.0 (0.75)

Speedup (Efficiency)

Single-frequency Parallel Scalability (FETI-DP)

	P1			P2		
n_p	M1	M3	M4	M1	M3	M4
2	1.00 (1.00)	X	X	1.00 (1.00)	X	1.00 (1.00)
4	1.05 (1.04)	1.00	1.00 (1.00)	1.04 (1.01)	X	0.95 (0.84)
8	0.96 (0.86)	1.09	0.79 (0.81)	0.91 (0.91)	X	0.66 (0.60)
16	0.84 (0.81)	1.32	0.62 (0.63)	0.75 (0.74)	X	0.50 (0.48)
32	0.66 (0.65)	0.90	0.52 (0.52)	0.47 (0.46)	X	0.31 (0.26)

- fi xed total work (32 partitions)
- ’X’: lack of enough memory per node

Closing Remarks

- STARS3D: general purpose, yet efficient for linear *PDE*'s
- p-version superior for wave-dominated problems
- Error-analysis a must for reliable verification
- Domain-decomposition (FETI-DP) type approach leads to better scalability
- Ongoing and future efforts: transient problems, adaptivity
- new application/interests: seismic-acoustics, Schrödinger-equation

1. S. Dey, D. K. Datta, A parallel hp-FEM infrastructure for three-dimensional structural acoustics, *Int. J. Numer. Meth. Engg.*, (In press), 2006.
2. S. Dey, D. K. Datta, J. J. Shirron and M. S. Shephard, p-version FEM for structural acoustics with *a-posteriori* error estimation, *Comp. Meth. Appl. Mech. and Engg.*, 195, pp:1946-1957, 2006.
3. S. Dey, Evaluation of p-FEM approximations for mid-frequency elasto-acoustics. *J. of Comp. Acoustics*, Vol. 11, No. 2, pp:195-225, 2003.
4. S. Dey, J. J. Shirron and L. S. Couchman, Mid-frequency structural acoustic and vibration analysis in arbitrary, curved three-dimensional domains, *Computers & Structures*,
Vol. 79, No. 6, pp:617-629, 2001.
5. M. S. Shephard, S. Dey and J. E. Flaherty, A straightforward structure to construct shape functions for variable p-order meshes, *Comp. Meth. Appl. Mech. and Engg.*, 147, pp:209-233, 1997.

Contact: dey [at] pa.nrl.navy.mil, 202-767-7321 Thank you! Questions ?